CrossMark
click for updates

Virus-Like Particles Displaying Trimeric Simian Immunodeficiency Virus (SIV) Envelope gp160 Enhance the Breadth of DNA/Modified Vaccinia Virus Ankara SIV Vaccine-Induced Antibody Responses in Rhesus Macaques

Smita S. Iyer,[a] Sailaja Gangadhara,[a] Blandine Victor,[a] Xiaoying Shen,[b] Xuemin Chen,[c] Rafiq Nabi,[d] Sudhir P. Kasturi,[e] Michael J. Sabula,[a] Celia C. Labranche,[f] Pradeep B. J. Reddy,[a] Georgia D. Tomaras,[b] David C. Montefiori,[f] Bernard Moss,[g] Paul Spearman,[c] Bali Pulendran,[e] Pamela A. Kozlowski,[d] Rama Rao Amara[a]

Department of Microbiology and Immunology, Emory Vaccine Center, Yerkes National Primate Research Center, Emory University, Atlanta, Georgia, USA[a]; Duke Human Vaccine Institute, Duke University Medical Center, Durham, North Carolina, USA[b]; Department of Pediatrics, Emory University School of Medicine, Atlanta, Georgia, USA[c]; Department of Microbiology, Immunology, and Parasitology, Louisiana State University Health Sciences Center, New Orleans, Louisiana, USA[d]; Department of Pathology and Laboratory Medicine, Emory University School of Medicine, Emory University, Atlanta, Georgia, USA[e]; Department of Surgery, Duke University Medical Center, Durham, North Carolina, USA[f]; Laboratory of Viral Diseases, National Institute of Allergy and Infectious Diseases, National Institutes of Health, Bethesda, Maryland, USA[g]

ABSTRACT The encouraging results of the RV144 vaccine trial have spurred interest in poxvirus prime-protein boost human immunodeficiency virus (HIV) vaccine modalities as a strategy to induce protective immunity. Because vaccine-induced protective immunity is critically determined by HIV envelope (Env) conformation, significant efforts are directed toward generating soluble trimeric Env immunogens that assume native structures. Using the simian immunodeficiency virus (SIV)-macaque model, we tested the immunogenicity and efficacy of sequential immunizations with DNA (D), modified vaccinia virus Ankara (MVA) (M), and protein immunogens, all expressing virus-like particles (VLPs) displaying membrane-anchored trimeric Env. A single VLP protein boost displaying trimeric gp160 adjuvanted with nanoparticle-encapsulated Toll-like receptor 4/7/8 (TLR4/7/8) agonists, administered 44 weeks after the second MVA immunization, induced up to a 3-fold increase in Env-specific IgG binding titers in serum and mucosa. Importantly, the VLP protein boost increased binding antibody against scaffolded V1V2, antibody-dependent phagocytic activity against VLP-coated beads, and antibody breadth and neutralizing antibody titers against homologous and heterologous tier 1 SIVs. Following 5 weekly intrarectal SIVmac251 challenges, two of seven DNA/MVA and VLP (DM+VLP)-vaccinated animals were completely protected compared to productive infection in all seven DM-vaccinated animals. Vaccinated animals demonstrated stronger acute viral pulldown than controls, but a trend for higher acute viremia was observed in the DM+VLP group, likely due to a slower recall of Gag-specific CD8 T cells. Our findings support immunization with VLPs containing trimeric Env as a strategy to augment protective antibody but underscore the need for optimal engagement of CD8 T cells to achieve robust early viral control.

IMPORTANCE The development of an effective HIV vaccine remains a global necessity for preventing HIV infection and reducing the burden of AIDS. While this goal represents a formidable challenge, the modest efficacy of the RV144 trial indicates that multicomponent vaccination regimens that elicit both cellular and humoral immune responses can prevent HIV infection in humans. However, whether protein immunizations synergize with DNA prime-viral vector boosts to enhance cellular and humoral immune responses remains poorly understood. We addressed this question in a nonhuman primate model, and our findings show benefit for sequential protein immunization combined with a potent adjuvant in boosting antibody titers induced by a preceding DNA/MVA immunization. This promising strategy can be further developed to enhance neutralizing antibody responses and boost CD8 T cells to provide robust protection and viral control.

W ith over 2.5 million new human immunodeficiency virus (HIV) infections per year, the majority in resource-poor countries with limited access to antiretroviral therapy, an effective HIV vaccine continues to remain among the most promising and safe strategies for preventing infection and reducing the burden of AIDS (1). To date, there have been six HIV vaccine efficacy trials that tested four different vaccine concepts. Only the RV144 trial showed a modest level of efficacy (2), and immune correlate analyses have yielded critical insights into immune determinants of vaccine-induced protection against HIV (3). Together with experimental data from rhesus models of HIV, these data underscore two key elements of vaccine efficacy: the induction of robust and long-lasting antibodies (Abs) against the envelope glycoprotein (Env) with potent neutralizing and effector functions to prevent the acquisition of infection and the induction of cytolytic T cell

responses against Gag proteins for controlling viral replication in the event of infection (4, 5). Consequently, vaccine strategies that

engender both humoral and cellular immune responses, including elicitation of B cell helper CD4$^+$ T follicular helper cells (T$_{FH}$) that are necessary for generating persistent antibody, are the focus of intense research.

In this regard, there is strong interest in multicomponent HIV vaccine platforms whose constituents work synergistically to engage multiple arms of the immune system. Such an approach could comprise recombinant plasmid DNA and live replication-defective viral vectors to induce robust cellular responses. Poxvirus vectors such as modified vaccinia virus Ankara (MVA) stimulate dendritic cells and induce appropriate inflammatory signals to elicit strong CD8 and CD4 T cell responses, especially as booster immunizations (6, 7). The latter could play a critical role in engaging germinal center B cells for fostering high-quality antibody, which subsequently can be boosted by Env protein immunizations.

As described previously, our DNA and MVA constructs are designed to present Env as native trimers on noninfectious virus-like particles (VLPs) expressed on the cell surface upon vaccination (8). This strategy is designed to focus the humoral response on trimer-specific antibodies present on the VLP. In preclinical and clinical studies, DNA/MVA (DM) vaccination elicits strong cellular and humoral immune responses (9, 10). A critical step toward strengthening this vaccine platform is to augment the humoral response to protective epitopes induced by the DNA/MVA vaccine. Protein immunogens are ideal for this purpose; however, it is critical to use Env protein immunogens that form stable trimers and assume a native Env conformation. To this end, recently developed SOS I559P gp140 (SOSIP) Env trimers have shown promise in inducing autologous neutralizing antibodies against hard-to-neutralize HIV isolates, and more work needs to be done in this direction (11, 12). Here, we took a different approach and determined whether the magnitude and quality of antibody responses induced by a DNA/MVA vaccine can be further augmented by boosting with a VLP protein immunogen displaying trimeric Env on the surface. Such a regimen would also provide insight into the value of extended protein immunizations in augmenting waning antibody titers.

We addressed these questions in the context of a simian immunodeficiency virus SIVmac239 (SIV239) DNA prime-SIV239 MVA boost followed by a late boost with VLPs containing SIV239 gp160 and Gag pr55. To enhance immunogenicity, the VLP immunogen was administered with potent nanoparticle-encapsulated Toll-like receptor 4/7/8 (TLR4/7/8) adjuvants. We report that a late trimeric gp160 boost induced a robust recall of binding antibody titers against gp140 and the scaffolded SIV239 V1V2 protein and homologous and heterologous tier 1 neutralization titers. The VLP boost also potently increased mucosal IgA and IgG responses and generated new epitope specificities, resulting in significantly enhanced antibody breadth. Together, these data provide novel insights into cellular and humoral immune responses elicited by a combination of viral vector and protein immunizations.

MATERIALS AND METHODS

Ethics statement. All animal protocols were approved by Emory University Institutional Animal Care and Use Committee (IACUC) protocol YER-2002343. All animal experiments were conducted in strict accordance with USDA regulations and recommendations for conducting experiments in accord with the highest scientific, humane, and ethical prin-

ciples, as stated in the *Guide for the Care and Use of Laboratory Animals* (13). Animals were housed in pairs in standard nonhuman primate cages. Animals received standard primate feed (Purina monkey chow) as well as fresh fruit and enrichment daily and had free access to water. Upon infection, animals were housed singly. Immunizations, infections, blood draws, and biopsy procedures were performed under anesthesia by trained research staff.

Animals. Twenty-four male Indian rhesus macaques were included in this study, 14 of which were immunized as described below. Animals ranged in age from 2 to 4 years and ranged in weight from 3 to 6 kg at the start of the study. Animals were negative for simian T cell lymphotropic virus, herpes B virus, simian retrovirus type D (SRV-D), and SIV at study commencement. None of the animals expressed Mamu class 1 alleles B08 and B17. The vaccine and control groups had 3 Mamu A*01 animals each. Animals from experimental groups were randomized into four sampling groups for immunization, challenges, and sampling of blood and tissue biopsy specimens. All animals were housed at the Yerkes National Primate Research Center (YNPRC) in Atlanta, GA, and treated in accordance with YNPRC IACUC regulations.

Study design, immunogens, and immunizations. The vaccine study consisted of two experimental groups; all 14 vaccinated animals received two CD40L-adjuvanted DNA primes (D) (0 and 8 weeks) followed by two MVA boosts (M) (16 and 32 weeks) (DDMM regimen). To determine whether an extended protein boost after the second MVA administration augmented antibody responses, 7 of the 14 animals received a VLP protein boost at week 76. The DNA immunogen expressed SIV239 Gag-Pol, Env, Tat, and Rev and rhesus macaque membrane-anchored CD40L (14) and was delivered at 3 mg/dose. The MVA immunogen expressed SIV239 Gag, Pol, and Env and was delivered at a 10^8 PFU/dose (15, 16). Protein vaccination consisted of purified VLPs (containing 50 μg gp160 Env and 1.5 mg Gag) premixed with poly(D,L-lactic-coglycolic acid) (PLGA)-based nanoparticle-encapsulated monophosphoryl lipid A (MPL) (TLR4 agonist) (50 μg) and R848 (TLR7/8 agonist) (750 μg) adjuvants prior to vaccination. Briefly, 200 μl of PLGA nanoparticles containing the respective adjuvants was admixed with 1 ml of VLPs by mild vortexing, followed by gently pipetting the mixture up and down prior to vaccination. The prepared inoculum was stored on ice until the time of inoculation. DNA and MVA immunizations were delivered in phosphate-buffered saline (PBS) intramuscularly in a single shot in the outer thigh. VLPs plus TLR4/7/8 adjuvants were administered subcutaneously behind the knee.

SIV infection. Animals were challenged with SIVmac251 intrarectally on a weekly basis for a maximum of 5 weeks or until detection of plasma viremia at levels above 250 copies/ml for two consecutive weeks. Infection with SIVmac251 (day 8) (7.9.10 virus stock from Nancy Miller at the NIH) was performed by using a 1-ml slip tip syringe containing 1 ml of SIVmac251 at 200 50% tissue culture infective doses (TCID$_{50}$). The syringe was inserted gently ~4 cm into the rectum, the plunger was depressed to instill the virus, and the animal was returned to the cage in a prone position.

Sample collection and processing. Peripheral blood mononuclear cells (PBMCs) were isolated from whole blood collected into sodium citrate tubes and isolated by density gradient centrifugation according to standard procedures, as described previously (15). PBMCs were isolated, counted, and utilized for various assays within 6 h of blood collection. After determination of cell counts, cells were used immediately or cryopreserved by using standard techniques. Cell viability in PBMC suspensions was determined to be above 90%. Rectal secretions were collected with and eluted from premoistened Weck-Cel sponges as previously described (17).

Linear epitope specificity. The linear epitope specificity of the antibodies was determined by profiling serum IgG responses against linear epitopes representing full-length SIV239 Env in a peptide microarray, as described previously (18). Sera from baseline, 2 weeks after the second MVA immunization, and 2 weeks after VLP immunization were examined. The peptide library consisted of 15-mer peptides overlapping by 12

covering SIVmac239 gp160. Serum was tested at a 1:50 dilution against slides (slide lot JPT 2413) coated with a library of peptide probes. A secondary goat anti-human fluorescent IgG antibody was added to tag peptide-bound serum antibodies, and slides were scanned (photomuliplier tube [PMT] setting 660, with 100% power) to yield fluorescence intensity values for each probe [19]. Final intensity values were computed after baseline subtraction, and the maximum binding for defined epitopes was determined based on the highest level of binding to a single peptide within the epitope region.

Binding antibodies. Concentrations of serum IgG binding antibodies to recombinant SIVmac239 gp140 (Immune Technology) or trimeric gp120 were measured by using gp140-coated plates or SIV239 VLPs captured on concanavalin A (ConA)-coated plates, respectively, as described previously [20, 21]. Concentrations of antibodies to SIVmac251 recombinant gp140 (rgp140) (Immune Technology) and total IgA and IgG in rectal secretions were measured by an enzyme-linked immunosorbent assay (ELISA) as previously described [22]. All samples intended for IgA antibody analysis were first depleted of IgG by using protein G-agarose (GenScript) as described previously [17]. Concentrations of gp140-specific IgA or IgG in secretions were divided by the total concentration of IgA or IgG to obtain the specific activity. Secretions were considered antibody positive if the specific activity was greater than or equal to the mean specific activity plus 3 standard deviations (SD) measured in secretions collected at baseline.

A customized binding antibody multiplex assay (BAMA) [23] was used in the Kozlowski laboratory to measure antibodies to recombinant SIVmac251 gp120 (Immune Technology), gp70-V1V2mac239 [24] (from D.C.M.), SIV p55gag (a gift from Francois Villinger, New Iberia Research Center), and HIV-2 gp36 (Prospec), which has 85% homology to the SIV gp41 ectodomain [25]. Each viral protein was conjugated to carboxylated Luminex beads (Bio-Rad) by placing 1×10^7 beads into the upper chamber of an Ultrafree 0.1-μm centrifugal filter unit (Millipore), washing the beads with PBS, and then adding 5 mg/ml N-hydroxysulfosuccinimide (Pierce) and 5 mg/ml ethyl-3-[3-diethylaminopropyl]carbodiimide hydrochloride (Sigma) in 0.1 M Na phosphate buffer (pH 6.2). After 20 min, the beads were washed and mixed at 900 rpm in an Eppendorf MixMate vortexer with 100 μg of protein that had been dialyzed in PBS. After 2 h, the beads were washed, resuspended in PBS containing 1% bovine serum albumin (BSA) and 0.05% azide, and counted in a hemocytometer. Assays were performed by using 2 panels of beads: gp120 and gp36 (panel 1) and V1V2 and p55 (panel 2). For each assay, 2,500 beads expressing each protein were added in a final volume of 25 μl to wells of a blocked, low-protein-binding, 96-well white plate (Costar), which contained 25 μl of serum and a standard that had been diluted in PBS containing 1% BSA, 0.05% Tween 20, and 0.05% azide (assay buffer). For IgG assays, the standard was IgG purified from pooled serum of SIV-infected macaques. For IgA assays, the standard was IgG-depleted serum from SIV-vaccinated/infected macaques [22]. All standards had been previously calibrated by an ELISA as described previously [26] and were adjusted in the bead assay mixture to achieve test sample concentrations similar to those obtained in ELISAs. After overnight mixing at 4°C, the plate contents were transferred onto a Durapore 96-well filtration plate (Millipore) and washed 4 times with PBS containing 0.05% Tween 20 in a BioTek ELx50 washer. The beads were mixed with 100 μl of 2 μg/ml biotinylated goat anti-monkey IgA or IgG (Rockland) for 30 min at room temperature, washed, and then treated with 100 μl of a 1/200 dilution of Neutralite-phycoerythrin (SouthernBiotech) in assay buffer. After 30 min at 900 rpm, the beads were washed, and the plastic tray on the bottom of the plate was removed. The filtration plate was then placed on top of the white plate. Beads were transferred back to the white plate by mixing with 100 μl of assay buffer, puncturing the filters with pipette tips, and then centrifuging the plates at 2,300 $\times$ g for 5 min. The beads were briefly mixed at 700 rpm on a rotating platform and then analyzed for fluorescence with a Bioplex 200 system (Bio-Rad). Concentrations of antibody were interpolated from standard curves constructed by using Bioplex Manager software.

Neutralization antibody responses. The SIV-specific neutralization antibody response was measured as a function of the reduction in luciferase reporter gene expression levels after a single round of infection in TZM-bl cells, as described previously [27]. Neutralization against homologous SIVmac251.6 (tier 1) and SIVmac251.30 (tier 2) and heterologous SIVsmE660/CP3C-P-48 (tier 1) and SIVsmE660/CR54-PK-2A5 (tier 2) was measured at peak and memory time points following the second MVA immunization and VLP boost. Values were considered positive for neutralization based on the criterion of >3× background signal with the negative-control virus simian virus amphotropic murine leukemia virus (SVA-MLV).

Antibody-dependent phagocytosis (ADP). Phagocytosis assays were performed as described previously [28], with the modifications noted below. Briefly, 1×10^9 1-μm Neutravidin Fluorospheres (Invitrogen) were labeled with 7 μg biotinylated recombinant SIV gp120mac251 (Immune Technology) or 5 μg biotinylated concanavalin A (vector) followed by 10 ml of VLP-containing medium produced by transfection of 293T cells with SIV DNA, as described above. After washing, 1×10^7 beads per well were added to V-bottom plates containing triplicate serial dilutions of heat-inactivated serum that had been absorbed against 293T cells. THP-1 cells (2×10^4 per well) were then added. After 6 h at 37°C in 5% CO_2, the cells were washed with Ca^{2+}/Mg^{2+}-free Dulbecco's PBS (DPBS) and incubated for 10 min with 50 μl of 0.05% trypsin-EDTA (Gibco). The cells were washed in DPBS, resuspended in 1% paraformaldehyde, and analyzed for fluorescence. The score was calculated as described previously [28], by multiplying the number of bead-positive cells by their median fluorescence intensity. To obtain the score ratio [29], the average score for the test samples was divided by the average score for naive monkey serum at the same dilution.

Plasma SIV RNA load. The SIV copy number was determined by using quantitative real-time PCR as previously described [14]. All PCRs were performed in duplicates, with a limit of detection of 60 copies per reaction.

Flow cytometry. Prior to intracellular staining for cytokines, fresh PBMCs were stimulated with peptide pools of Gag and Env for 5 h in the presence of brefeldin A (Golgi Plug; BD Biosciences, San Jose, CA). Unstimulated cells from each animal served as a negative control, and PBMCs stimulated with phorbol myristate acetate-ionomycin served as positive controls. Cells suspensions were first stained with the Live/Dead Near-IR dead-cell stain from Molecular Probes, Invitrogen (Grand Island, NY), in PBS containing 2% fetal bovine serum (FBS) (fluorescence-activated cell sorter [FACS] buffer) for 30 min at 4°C. Intracellular staining was performed after cells were fixed with Cytofix/Cytoperm (BD Biosciences, San Jose, CA), followed by permeabilization with BD Perm/Wash buffer according to the manufacturer's instructions. Cells were stained in Perm/Wash buffer with CD3 (SP34-2), CD4 (OKT4), CD8 (SK1), gamma interferon (IFN-γ) (B27), tumor necrosis factor alpha (TNF-α) (MAb11), interleukin-2 (IL-2) (MQ1-17H12), and IL-21 (3A3-N2.1), from BD Pharmingen, at 4°C for 45 min. After two washes, samples were acquired on an LSR Fortessa instrument (BD Biosciences), and 500,000 total events were collected for each sample. Data were analyzed by using FlowJo software vX.0.7 (Tree Star, Inc., Ashland, OR). Dead cells were excluded from the analysis.

Statistical analysis. Statistical analysis was performed by using GraphPad Prism v5.0. A two-tailed nonparametric t test was used for all comparisons unless otherwise specified. Spearman correlation was used to determine associations between variables. Statistical significance was set at a P value of <0.05.

RESULTS

Production and characterization of SIV239 VLPs. The decline in Env antibody titers postvaccination and the associated increase in HIV acquisition risk in RV144 vaccinees spurred interest in ex-
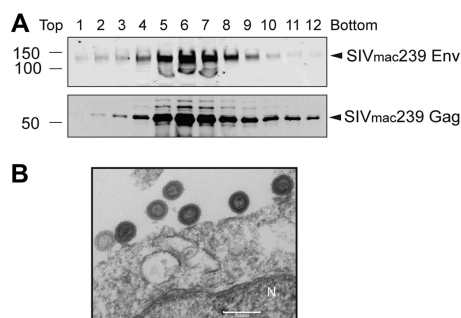
FIG 1 Characterization of SIV VLPs produced in 293F cells. (A) Western blot analysis of sucrose fractions collected from a 20 to 60% sucrose gradient. Supernatants collected from 293F producer cells were pelleted through 20% sucrose, resuspended, and loaded onto a 20 to 60% gradient. Twelve fractions were collected from top to bottom. (B) Transmission electron micrograph of SIV VLPs budding from 293F producer cells. N, nucleus.

tended protein boosting regimens as a strategy to augment waning Env titers and enhance vaccine efficacy (30). The objective of the present study was to determine whether an extended protein boost contributes significantly to enhancing antibody titers induced by a DNA prime-MVA boost immunization. We evaluated this question by employing DNA and MVA constructs designed to express trimeric Env on VLPs *in vivo*. In an effort to augment conformation-dependent Env antibody responses, we employed a VLP protein boost. The VLP protein immunogen was generated by using an inducible 293F SIV Gag-Env stable production cell line. Codon-optimized SIVmac239 Gag and Env genes were synthesized (GenScript) and cloned into the pcDNA4/TO and pcDNA5/TO vectors (Thermo Fisher Scientific), respectively. 293F cells were transfected with both vectors and selected by culture in zeocin and puromycin, followed by single-cell cloning and expansion of high-producer clones. VLP production was induced by the addition of doxycycline for 48 h, after which VLPs were pelleted through a 20% sucrose cushion. Purified VLPs were resuspended in PBS and were quantified by p27 and gp120 ELISAs for Gag and Env contents prior to immunization. VLP production lots were characterized on a 20 to 60% sucrose gradient, followed by Western blotting (Fig. 1A). As expected, fractions 5 to 7 (density from 1.14 to 1.16 g/cm^3) were enriched in VLPs, as measured by the enrichment of Env and Gag in these fractions. Electron micrograph analysis of transfected cells confirmed the presence of budding VLPs on the cell membrane (Fig. 1B).

Study design. Fourteen rhesus macaques were primed intramuscularly with 3 mg of CD40L-adjuvanted plasmid DNA expressing SIVmac239 Gag, protease, reverse transcriptase (RT), Env gp160, Tat, and Rev and coexpressing macaque CD40L at 0 and 8 weeks (14) (Fig. 2A). Booster immunizations comprised recombinant MVA expressing SIVmac239 Gag, protease, RT, and Env gp150 administered intramuscularly at 10^8 PFU on weeks 16 and 32. After a 24-week rest period, seven animals were challenged intrarectally at weekly intervals with 200 $TCID_{50}$ (1.16×10^7 copies of viral RNA) of SIVmac251 for 5 weeks. Animals that tested positive for SIV Gag at >250 copies/ml plasma for two consecutive weeks were not challenged further. Unvaccinated control animals were similarly challenged. The remaining seven animals received a subcutaneous booster immunization with SIVmac239 VLPs containing Env gp160 (50 μg) and Gag (1.5 mg), together with PLGA-based nanoparticle (NP)-encapsulated MPL (TLR4

agonist) (50 μg) and R848 (TLR7/8 agonist) (750 μg) adjuvants at week 76 (31). Following a 12- or 20-week rest period, animals in the VLP group were challenged with the same SIVmac251 viral stock by using identical infection protocols. All animals were monitored for viral control and anti-SIV immune responses for 24 weeks following infection. Animals were male and negative for Mamu B*08 and B*17 alleles.

NP-adjuvanted VLP protein boost elicits strong recall of DNA/MVA-induced anti-Env binding Ab titers in sera. To evaluate humoral immune responses, serum samples were collected at peak and memory time points after each of the booster immunizations. Binding IgG antibody responses to homologous SIVmac239 Env gp140 were detected by an ELISA in all animals after the first MVA boost, with median peak titers of 10 μg/ml, and responses significantly increased after the second MVA immunization, with median peak titers of 175 μg/ml (Fig. 2B). These responses declined to a median of 35 μg/ml by 10 weeks and were maintained at these levels for the next 34 weeks. A single immunization with NP-adjuvanted VLP protein robustly boosted gp140 titers by an average of 20-fold (range, 12- to 28-fold), resulting in median peak gp140 titers of 468 μg/ml, which significantly exceeded peak responses after the second MVA boost ($P < 0.01$) (Fig. 2C). Similar increases in binding antibody titers were also observed against Env gp160 derived from Triton X-100-dissociated VLPs and captured on ConA-coated plates (Fig. 2B and C), SIVmac251 gp120, and HIV-2 gp36, which is highly homologous to SIVmac251 gp41 (25) (Fig. 2D). Due to the high concentrations of Gag contained in the VLP immunogen, we measured antibody titers against the recombinant SIV239 Gag p55 protein (Fig. 2E) and observed a 17-fold increase in peak titers following the VLP boost (median of 70.3 μg/ml, compared to a median of 4.25 μg/ml after the second MVA boost; $P < 0.05$). Assessment of titers against gp140 and ConA-captured gp160 10 to 12 weeks following the second MVA and VLP boosts (memory of VLP) showed that the VLP boost significantly increased memory titers against ConA-captured gp160 but not against gp140 (Fig. 2F). These results demonstrated that VLPs displaying trimeric SIV Env induce a strong recall of SIV gp120-, gp41-, and Gag-specific antibody responses in serum.

NP-adjuvanted VLP protein boost elicits strong recall of serum antibody with neutralization and antibody-dependent phagocytosis activities. Next, we determined whether antibody-neutralizing activity was boosted after VLP immunization. We measured neutralization responses against homologous (SIVmac251) and heterologous (SIVsmE660) SIV isolates using a TZM-bl cell-based assay (27). While a response against harder-to-neutralize tier 2 homologous and heterologous viruses was not detected, the VLP boost augmented neutralization activity against tier 1 viruses relative to the second MVA vaccination (Fig. 3A and B). This was true at peak (week 2) as well as memory (weeks 8 to 10) time points (Fig. 3A and B). We also sought to evaluate associations between binding antibody titers and neutralizing antibody responses after MVA and VLP boosts; the data showed that neutralizing responses were highly correlated with the magnitude of gp140 binding titers at peak and memory time points after MVA immunization but not at the peak time point post-VLP boost (Fig. 3C). Indeed, neutralization responses were constant over a range of antibody titers in VLP-boosted animals, suggesting that neutralization activity did not increase in proportion to the increase in binding antibody titers following the VLP boost. Together, the
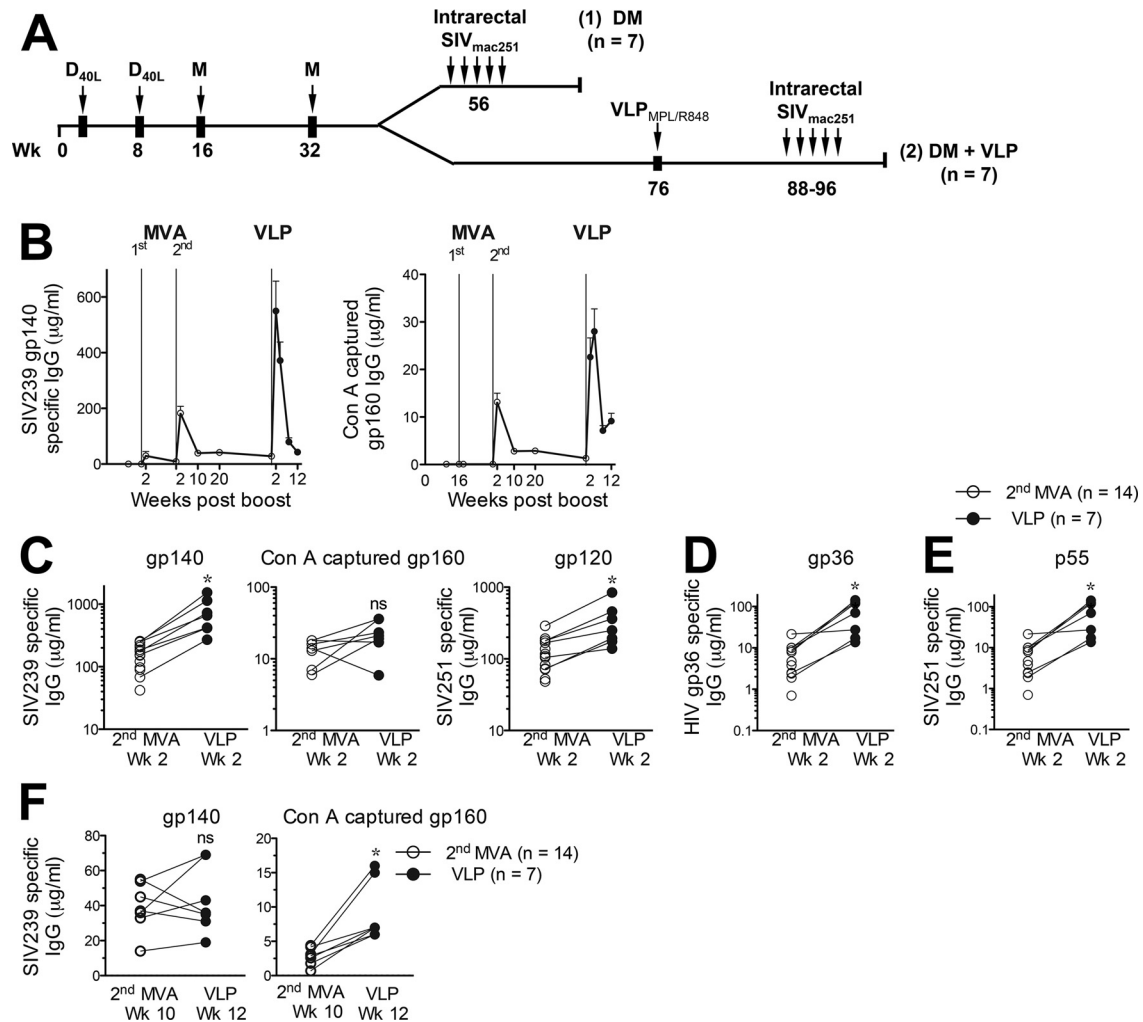
FIG 2 NP-adjuvanted VLP protein boost elicits strong recall of DNA/MVA-induced anti-Env binding Ab titers in sera. (A) Experimental design. (B) Kinetics of Env-specific binding after each booster immunization against soluble gp140 and ConA-captured VLP-derived gp160. Geometric means and standard errors of the means are shown. (C) Magnitude of gp140 or ConA-captured gp160 Env-specific IgG response 2 weeks after the second MVA immunization ($n = 14$) and 2 weeks after VLP immunization ($n = 7$) as determined by an ELISA (background, 0.07 µg/ml). (D) Magnitude of gp120-specific (background, 0.006 µg/ml) (*, $P < 0.05$) and HIV gp36-specific (highly homologous to SIV gp41) (background, 0.008 µg/ml) IgG responses as determined by using a BAMA. (E) Magnitude of SIV p55-specific IgG responses. (F) Comparison of antibody responses at the memory time point after the second MVA and VLP boosts. *, $P < 0.05$.

data demonstrate that the VLP protein boost effectively elicits a robust recall of DNA/MVA-induced neutralizing antibody responses.

We also evaluated whether nonneutralizing functional antibody responses were correspondingly boosted at the peak time point following VLP immunization. We measured antibody-dependent phagocytosis (ADP) against gp120 and VLP-coated beads in serum at the peak time points after the second MVA immunization and post-VLP immunization. We computed the phagocytic score by computing the ratio of ADP responses in vaccine sera to the response from naive monkey sera. Assessment of ADP responses using THP-1 monocyte-mediated capture of SIVmac251 gp120 or ConA-VLP-coated fluorescent beads (28) showed a significant increase at the peak time point post-VLP immunization relative to that at the peak time point after the second MVA immunization (Fig. 3D and E). The magnitude of ADP responses against gp120 and VLP-coated beads directly correlated with anti-gp120 binding antibody titers. Thus, our data

indicate that a VLP booster following DNA/MVA immunization induced antibodies that direct tier 1 neutralizing responses and ADP activity.

NP-adjuvanted VLP protein boost elicits strong increases in Env-specific IgG and IgA titers in rectal mucosa. We next sought to ascertain whether VLP immunization also boosted Env-specific antibody titers in the rectal mucosa. For this purpose, we assayed colorectal secretions nontraumatically using premoistened Weck-Cel sponges according to previously described protocols (17, 22). Total and Env-specific IgG and IgA responses were assessed at baseline and longitudinally after the second MVA and VLP boosts (Fig. 4). Responses were considered positive if the absorbance was greater than the mean plus 3 standard deviations of the absorbance of baseline samples. Based on this criterion, the cutoffs for absorbance were 0.03 for IgG and 0.23 for IgA responses in mucosa.

Similarly to serum IgG, the VLP boost induced a robust increase in mucosal gp140-specific IgG titers (Fig. 4A). The magni-
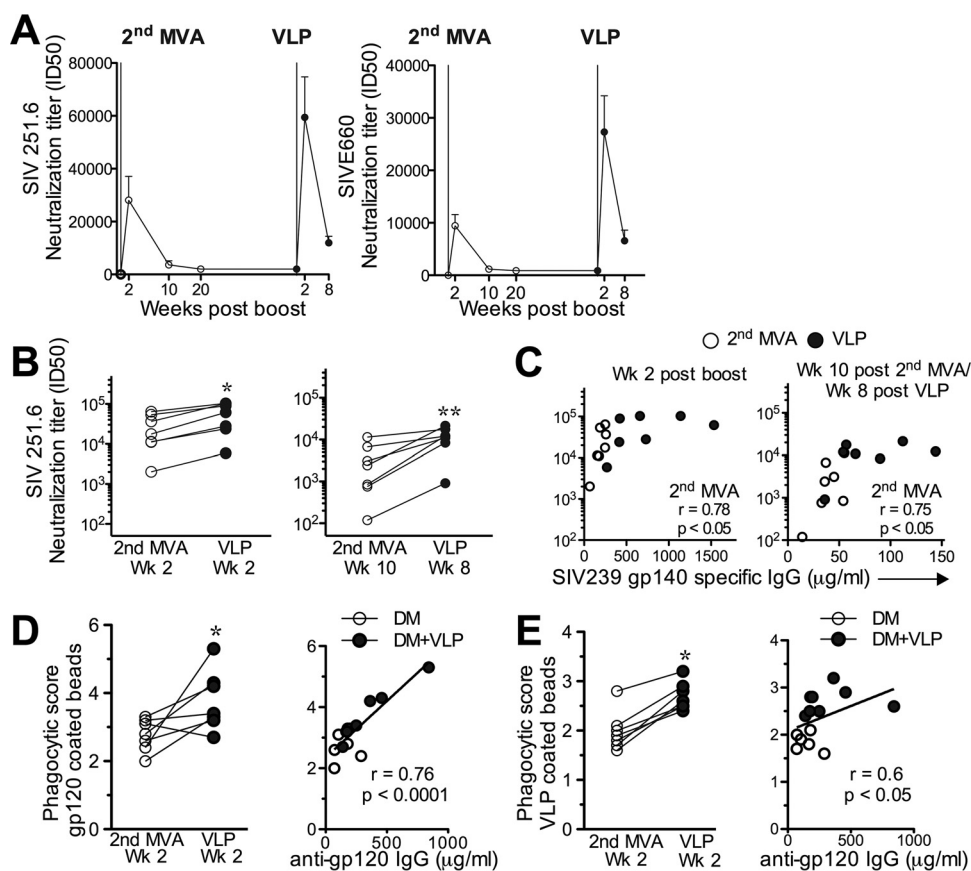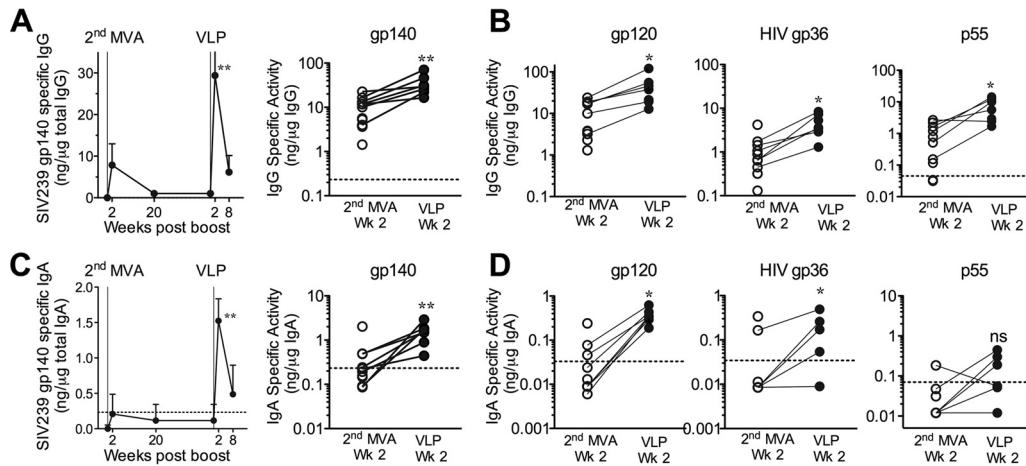
FIG 3 NP-adjuvanted VLP protein boost elicits strong recall of serum antibody with neutralization and antibody-dependent phagocytosis activities. (A) Kinetics of neutralization against homologous SIVmac251.6 and heterologous SIVsmE660 tissue culture laboratory-adapted (TCLA) tier 1 viruses, measured by using a TZM-bl cell-based assay. (B) Fold increase in neutralization titers at the peak time point after VLP immunization relative to the second MVA immunization (*, $P < 0.05$). (C) Scatter plots showing associations between gp140 binding titers and SIVmac251 neutralization responses in sera ($R^2 = 0.61$; *, $P < 0.05$ at peak). (D and E) Increase in phagocytosis scores (ADP score of vaccine sera/ADP score of naive monkey sera) measured against SIVmac251 gp120-coated beads at a 1:2,000 dilution of sera (E) and ADP score measured against SIV239 VLP-coated beads at a 1:200 dilution of sera in THP-1 monocytes at the peak time point post-VLP immunization compared to the peak time point after the second MVA immunization (E) (*, $P < 0.05$). Kinetic data show geometric means and standard errors of the means. ID50, 50% infectious dose.

tude of the IgG response 2 weeks after the VLP boost (median of 29.4 µg/ml) was 3.8-fold higher ($P < 0.01$) than the magnitude 2 weeks after the second MVA boost (median of 7.8). This increase in gp140-specific IgG titers was due to an increase in titers against both gp120 and gp41 (Fig. 4B). As expected, Env-specific mucosal IgG responses strongly correlated with systemic IgG responses ($P < 0.01$) (data not shown) (32). Similarly to the responses in sera, we found a significant increase in anti-Gag IgG titers in the rectal mucosa.

Peak SIV Env-specific IgA responses after the second MVA immunization were low and detectable in only 5/14 animals (median, 0.21 µg/ng total IgA). However, booster immunization with VLPs significantly enhanced mucosal IgA responses (median, 1.5 ng/µg total IgA) (Fig. 4C), resulting in peak titers that were, on average, 6-fold higher ($P < 0.01$) than those for the second MVA immunization. Consistently, IgA titers against gp120 and gp41 were significantly higher after VLP immunization than after the second MVA immunization (Fig. 4D). Measurement of gp140-specific IgA responses in sera showed that VLP immunization induced strong gp140-specific responses in the systemic compartment, which did not correlate with mucosal IgA responses (data

not shown). However, unlike the significant increase in Gag-specific IgG titers, we did not observe an increase in Gag-specific IgA titers in the mucosa. In summary, the data show robust induction of mucosal Env-specific IgG and IgA responses following VLP booster immunization.

NP-adjuvanted VLP protein boost enhances the breadth and dominance of IgG responses specific to linear Env peptides. Having established the robust induction of binding antibody responses after VLP immunization, we next determined whether the VLP boost changed the epitope specificity. For this purpose, we assessed Env-specific IgG responses to overlapping linear peptides (15-mers overlapping by 12) spanning the entire SIV239 gp160 protein. The intensity of binding to each peptide was determined at week 2 following the second MVA and VLP immunizations after baseline subtraction. The maximum binding intensity for each epitope was computed from the highest intensity of binding to a single peptide within the region. As described previously, the binding antibodies elicited after the second MVA immunization showed response rates (i.e., signal intensity value above 200) for linear epitopes comprising the V1b (85% responders), V2 (100%), C5 (71%), gp41 (100%), and Kennedy epitope (KE)

FIG 4 NP-adjuvanted VLP protein boost elicits strong increases in Env-specific IgG and IgA titers in rectal mucosa. (A) Kinetics of gp140-specific IgG in rectal mucosa. Scatter plots show increases in binding titers against gp140 (**, $P < 0.01$). (B) gp120- and HIV gp36 (highly homologous to SIV gp41)-specific IgG titers after VLP boost at the peak time point relative to the second MVA immunization, measured by a BAMA (*, $P < 0.01$). (C) Robust induction of gp140-specific IgA responses in rectal mucosa following the VLP boost (**, $P < 0.01$). (D) gp120- and HIV gp36-specific IgA titers after VLP boost at the peak time point relative to the second MVA immunization, measured by a BAMA (*, $P < 0.01$). Kinetic data are shown as geometric means and standard errors of the means.

(71%) regions of SIVmac239 gp160 (18). The breadth of the response to various regions of gp140 was highly correlated with the magnitude of gp140 binding titers: the animal with the lowest gp140 titers (68 μg/ml) showed responses to 3 regions, comprising the V1b, V2, and gp41-immunodominant (ID) regions, whereas animals with binding titers of >400 μg/ml showed responses to 8 to 10 regions. Figure 5A compares the antibody profiles expressed as median binding intensities at the peak time point after the second MVA immunization and after VLP immunization. Figure 5B shows the heat map aggregate of baseline-subtracted binding intensity values against the gp160 peptide for seven vaccinated animals at peak MVA and VLP time points. VLP immunization significantly increased the breadth of the response, with most new specificities being induced for the C1a and C1b regions (Fig. 5B). In addition, the magnitude of binding to the C5, V2, gp41-ID, and KE regions was significantly enhanced after the VLP boost (Fig. 5C).

Examination of the proportions of responses to different regions in the total gp160 array demonstrated that VLP immunization altered the specificity of the response from a V2-dominant response after the second MVA immunization to a KE-dominant response (Fig. 5D). While the mechanisms driving immunodominance to the KE region, situated in the cytoplasmic tail of gp41, after VLP immunization is not presently clear, it could be raised by looping out of the KE from a transfected cell *in vivo* or by the presence of disrupted VLPs in the vaccine preparation, as we have observed for our HIV VLP preparations *in vitro* (Fig. 5G).

We next determined whether antibody responses to gp70-scaffolded V1V2 antigens (Ags) were induced after VLP immunization. The data showed that the anti-gp70 V1V2 IgG antibody titer was increased in the sera of 4/7 animals after VLP immunization. The magnitude of V1V2 responses at the peak time point post-VLP immunization correlated with the magnitude of binding antibody titers to gp120 and gp140 (data not shown). Furthermore, reactivity to gp70-scaffolded V1V2 also directly correlated with the intensity of binding to V1b linear peptides (Fig. 5E). In rectal

mucosal secretions, we observed a significant enhancement in IgG-specific activity against V1V2 antigens, which was highly correlated with serum V1V2 responses (Fig. 5F). In summary, this comprehensive analysis demonstrated that a single booster immunization with NP-adjuvanted VLP protein resulted in an increased breadth of antibody responses, a shift in epitope dominance, and an increase in rectal IgG binding responses to the gp70-scaffolded V1V2 protein.

NP-adjuvanted VLP immunization enhances SIV-specific IFN-γ-centric CD4 T cell responses. After establishing the ability of a late protein boost to efficiently induce humoral immune responses, we next compared MVA and protein immunizations for the magnitude and quality of cellular responses. We assessed antigen-specific CD4 T cells by stimulating PBMCs at peak and memory time points following each boost with 15-mer peptide pools spanning SIVmac239 Gag and Env. Each of the three booster immunizations induced a strong recall of Gag- and Env-specific CD4 T cells, with responses after the first MVA immunization being significantly higher than those after the second MVA and VLP boosts (Fig. 6A and B). Stratifying Ag-specific responses by Gag and Env revealed an equivalent recall of Gag- and Env-specific CD4 T cell responses after VLP immunization relative to that induced after the second MVA immunization (Fig. 6B).

Next, we evaluated how a VLP protein boost altered the cytokine profile of antigen-specific CD4 T cells. CD4 T cells were examined for the production of IFN-γ, TNF-α, IL-2, and IL-21 after peptide stimulation. Boolean analysis revealed that ~20% of SIV-specific CD4 T cells produced all four cytokines after the second MVA boost, and this polyfunctional response was substantially reduced after VLP immunization. Indeed, the frequency of cells producing 3 or more cytokines was dramatically decreased after VLP immunization, and antigen-specific CD4 T cells were preponderantly IFN-γ producers, with a large fraction coproducing either TNF-α or IL-21. Whether this marked shift from a polyfunctional to a bifunctional cytokine profile was shaped by the adjuvant or is a feature of recall responses to multiple boosts is not clear. Temporal kinetics of vaccine-induced CD8 T cells showed
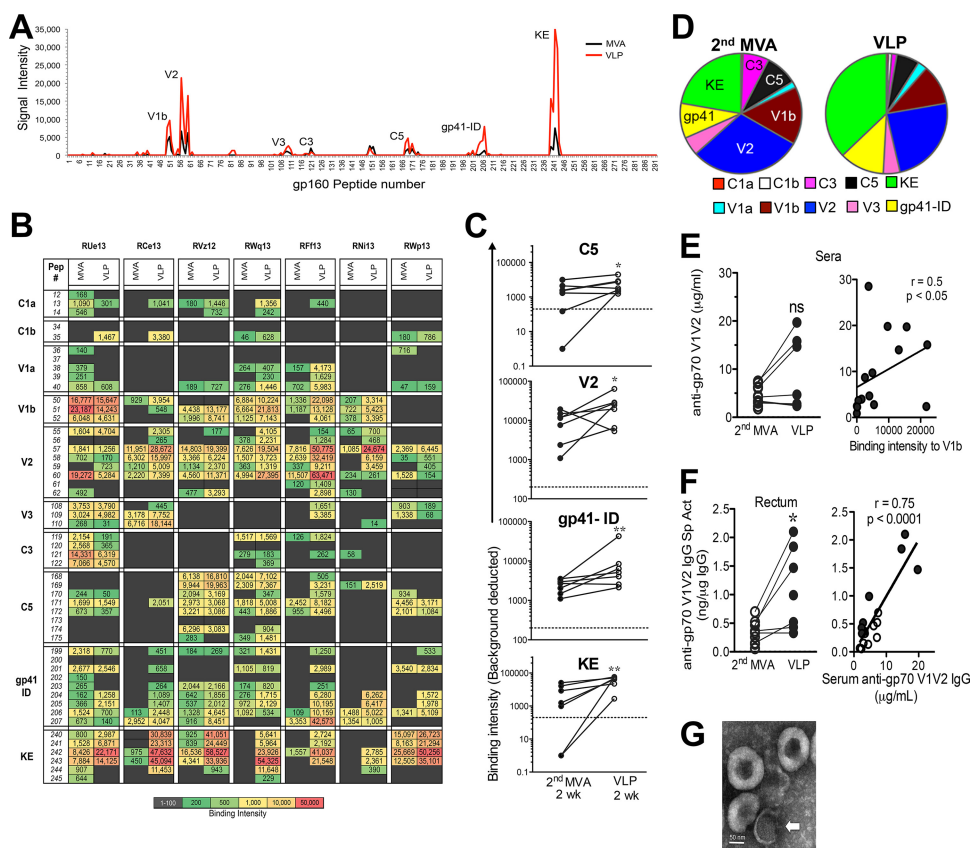
FIG 5 Breadth/epitope specificity after VLP immunization. Linear epitope mapping of sera was performed against a peptide library of 15-mers overlapping by 12 covering SIV239 gp160. (A) Signal intensity computed after baseline subtraction for defined regions of gp160 at the peak time point after the second MVA immunization and at the peak time point post-VLP immunization. (B) Heat map overview of signal intensity values for each region for 7 animals at peak MVA and VLP time points. Values of >200 are considered positive. (C) Increase in epitope specificity for C5, V2, gp41-ID, and KE regions after VLP boost (*, $P < 0.05$; **, $P < 0.01$). (D) Proportion of responses to different regions with a KE-dominant response after VLP boost. (E) Anti-gp70 V1V2 IgG titers in sera as measured by ELISAs correlate with binding intensity against the linear V1b peptide. ns, not significant. (F) Anti-gp70 V1V2 titers are significantly increased in mucosal secretions following VLP boost and correlate with responses in sera (*, $P < 0.05$). (G) Negative electron microscopy stain of VLPs from an HIV Gag construct showing an image of a broken VLP identified by a visible Gag protein lattice (arrow) together with three unbroken VLPs.

that VLP immunization did not boost DNA/MVA-induced memory CD8 T cells (Fig. 6D); the lack of anamnestic CD8 T cell responses after VLP immunization is consistent with the inefficiency of protein antigens in engaging the class I cellular machinery needed to elicit effective CD8 responses.

Effects of vaccination on acquisition and viral control. Next, we evaluated vaccine efficacy against a repeat, moderate-dose (200 TCID$_{50}$), intrarectal challenge with highly stringent SIVmac251 and observed that vaccination did not significantly delay acquisition (Fig. 7A). However, we noted some observations of interest. Of the unvaccinated controls, 40% were productively infected after the first challenge, the majority were infected after the second challenge, and all unvaccinated controls were infected after the fourth challenge. In the DM group, 30% of animals became infected after the first challenge, 80% became infected after the second challenge, and it took 5 challenges to infect the remaining animal. Inclusion of the VLP boost delayed acquisition, with 57% of animals in the DM plus VLP (DM+VLP) group becoming infected after the second challenge and 28% resisting infection (2/7 protected) (Fig. 7A). Of the two protected animals in this group, animal RWp13 showed a blip, with 90 SIV RNA copies/ml after the fourth challenge and remained below 60 copies after the fifth

challenge. Animal RUe13 showed apparent sterilizing protection, with viral copy numbers being below 60 copies during and subsequent to 5 challenges. Viral copy numbers in both animals remained at <60 copies of plasma SIV RNA for 24 weeks postinfection.

We next asked whether vaccine-induced humoral responses correlated with the acquisition of infection in either the DM or the DM+VLP group. Neither binding titers nor neutralization and nonneutralizing responses were significantly associated with acquisition. However, the magnitude of the Env IgG response to gp70-scaffolded V1V2 proteins at the peak time point postboost in sera was positively associated with a delay in acquisition in vaccinated animals (Fig. 7B).

Although neither vaccine regimen had a significant impact on acquisition, vaccination significantly aided in acute viral control (Fig. 7C). The analysis of viral loads was performed only on infected animals, and protected animals were not included. At 3 weeks postinfection, unvaccinated animals showed a robust peak in viremia ranging from 5.3 to 8 log RNA copies/ml, while the viral load in vaccinated animals ranged between 2 and 6 log RNA copies/ml plasma. However, we noted that the peak viral load in VLP-boosted groups was higher, with significantly higher viral loads at
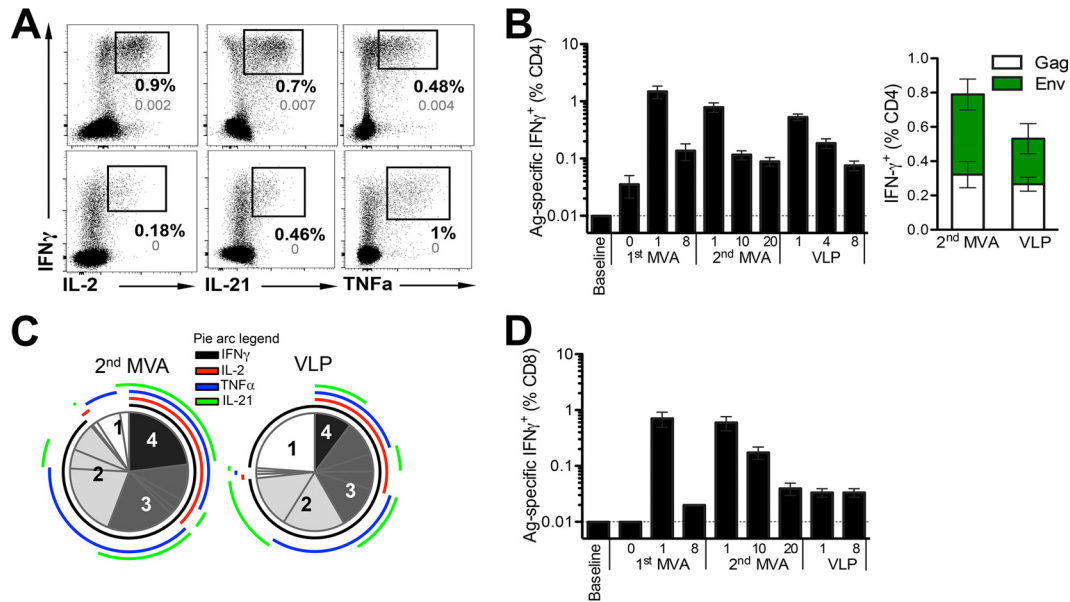
FIG 6 NP-adjuvanted VLP immunization elicits SIV-specific IFN-γ-centric CD4 T cell responses. (A) Flow plots showing coproduction of IFN-γ with IL-2, IL-21, and TNF-α in PBMCs after stimulation with Gag peptide pools 1 week after the second MVA immunization and 1 week post-VLP immunization. The background frequency from unstimulated PBMCs is shown in gray. (B, left) Kinetics of Gag- and Env-specific CD4 T cell responses (geometric means and standard errors of the means) over the course of immunization. (Right) Magnitude of IFN-γ-positive (IFN-γ[+]) responses to Gag and Env antigens (geometric means and standard errors of the means) 1 week after the second MVA immunization and 1 week post-VLP immunization. (C) Boolean gating analysis of cytokine-positive populations after stimulation for production of IFN-γ, IL-2, TNF-α, or IL-21. Each responding cell is assigned to 1 of 15 possible combinations of IFN-γ, IL-2, TNF-α, or IL-21, and data are presented as a pie chart illustrating polyfunctionality. (D) Ag-specific CD8 T cells are not recalled after VLP immunization. The bar graph shows kinetics of Gag- and Env-specific CD8 T cell responses (geometric means and standard errors of the means) over the course of immunization.

week 1 (Fig. 7D), while at week 2 and 3, a trend for higher viral loads was observed (Fig. 7D). We did not observe an association with Mamu A*01 status (Fig. 7D, green circles) and peak viremia. By week 7, VLP-boosted animal achieved viral control similarly to the DM groups, and at week 24, animals in the DM+VLP group showed significantly lower viral loads than did non-Mamu A*01 animals in the DM group (Fig. 7D). Unexpectedly, we observed viral control in some of the unvaccinated animals by 24 weeks postinfection (Fig. 7E).

Immune correlates of viral control. To gain an understanding of how vaccine-induced immune responses influenced early viral control, we examined SIV-specific T cell and antibody responses following infection. Vaccinated animals showed an overall higher frequency of Gag- and Env-specific CD8 T cells at weeks 3 and 7 postinfection than did unvaccinated controls (Fig. 8A). However, at week 3 postinfection, VLP-boosted animals showed on average lower frequencies of SIV-specific CD8 T cells than did the DM group (Fig. 8A). Because VLP immunization did not boost DNA/MVA-induced memory CD8 T cells, it is possible that the longer time interval between the final MVA boost and challenge in VLP-boosted animals contributed to the slower recall of Gag-specific CD8 T cells following infection. Indeed, the magnitude of the Gag-specific CD8 T cell response at week 3 postinfection was significantly associated with acute viral control in both vaccinated and control animals.

Similarly, the magnitudes of SIV-specific CD4 T cell responses were higher in vaccinated animals and were significantly higher in the DM group than in the DM+VLP group at the peak time point (Fig. 8B). The magnitude of the Gag-specific CD4 T cell response

was inversely associated with viral load in control animals, consistent with virus-induced CD4 depletion. Assessment of gp140-specific IgG responses showed robust recall in vaccinated groups at significantly higher titers than those in controls. Unlike the T cell responses, the DM+VLP group mounted gp140 responses that were equivalent to those mounted by the DM group at weeks 3 and 7 postinfection (Fig. 8C). Titers peaked at week 7 in unvaccinated controls, and the magnitude of titers was inversely associated with viral load. In summary, the data show that DM+VLP immunization resulted in a trend for better protection and evidence for better viral control at week 24 than for the DM group.

DISCUSSION

In the present study, we investigated the immunogenicity and efficacy of a vaccine platform consisting of sequential immunizations with DNA, MVA, and protein vaccines, each displaying trimeric SIV Env on the surface of VLPs. We made three main observations. First, boosting with TLR4/7/8-adjuvanted VLP protein induced a significant enhancement of systemic antibody titers; induced new epitope specificities, resulting in an enhanced breadth of antibody responses, and induced tier 1 neutralization titers. Second, mucosal antibody responses were strikingly enhanced. Third, nonneutralizing ADP responses were significantly boosted after VLP immunization. Notably, two out of seven VLP-boosted animals showed complete protection against a highly stringent intrarectal SIVmac251 challenge, compared to no protection in the DM group. VLP-boosted animals, however, showed poorer acute viral control due to a slower recall of CD8 responses postinfection. These data offer optimism for VLP protein im-
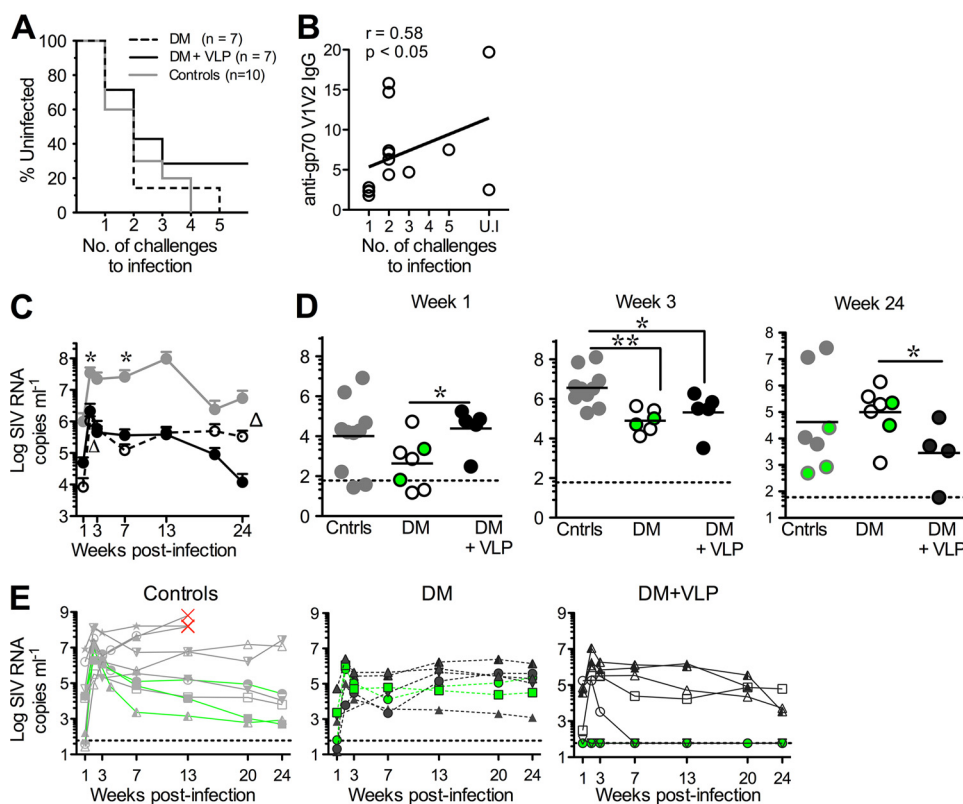
FIG 7 Acquisition and viral control in DM and DM+VLP vaccine regimens. (A) Acquisition curves against intrarectal SIVmac251 challenge. (B) SIV239 anti-gp70 V1V2 IgG titers (micrograms per milliliter) in serum are correlated with protection. UI, uninfected (C) Kinetics of viral loads after productive infection (* indicates significant differences between controls and each of the vaccinated groups, with a P value of <0.05; $\triangle$ indicates significant differences between vaccine groups, with a P value of <0.05; and ** indicates a P value of <0.01). (D) Scatter plots showing virus control in vaccinated animals at week 1, week 3, and week 24 postinfection. (E) Viral load kinetics in control, DM, and DM+VLP groups. The red X's in the control group for three animals indicate euthanasia due to the development of AIDS-related complications. Data for A*01 animals in each of the groups are shown in green. Kinetic data are shown as medians and standard errors of the means for each group.

munogens as booster vaccines but underscore the importance of utilizing optimal Env constructs in the correct conformation and the use of appropriate adjuvants and/or vectors targeting CD8 T cells for robust early viral control.

Much needs to be understood about the mechanism of generation of broadly neutralizing antibodies, and intense efforts are directed toward Env immunogen design to achieve this goal. In the present study, VLP immunization with Env gp160 induced a robust boost of binding and neutralizing titers against tier 1 SIV isolates but not against extremely neutralization-resistant SIVmac251. In fact, to our knowledge, only a live attenuated SIV vaccine (SIV239 delta3) generated neutralizing activity against SIVmac251 but only at very low levels and much later in infection (33). Based on this, it is difficult to ascertain the potential of a VLP protein boost to generate neutralizing antibody responses against tier 2 viruses, and HIV Env rather than SIV Env may serve as an ideal immunogen to address this question.

There is substantial evidence firmly establishing that the generation of antibodies against the variable V1V2 regions of Env may be protective (34). Previous studies using SIV immunogens demonstrated a strong IgG response to gp70-scaffolded V1V2 antigens as a correlate of protection against SIVmac251 challenge (35, 36). This was consistent with correlates of protection in the RV144 trial (36). Encouragingly, in our study, we observed a significant boost

of binding IgG titers against gp70-scaffolded V1V2 in rectal secretions. Importantly, we also observed a significant correlation between the anti-V1V2 response in sera and protection against SIVmac251, highlighting the utility of VLP proteins as booster immunogens for DNA and viral vectors.

Our analysis of the linear epitope specificity of binding antibody responses revealed that VLP immunization boosted the response to epitopes that were primed by DNA/MVA vaccination and, in addition, generated new epitope specificities. However, unexpectedly, VLP immunization induced a preponderance of responses to the KE region, which resulted in a shift in epitope dominance from V2 to the KE region relative to the second MVA immunization. The KE is situated in the cytoplasmic tail of gp41, and the mechanisms by which this represents a dominant epitope after VLP immunization are not entirely clear. Our preliminary data using HIV VLP constructs strong suggest that the presence of broken VLPs presenting Env stumps could mediate such a response. Importantly, the present data indicate that responses to the KE region do not predict antibody neutralization or vaccine efficacy, suggesting that improvements in VLP immunogen design to mask immunodominant responses to the KE region and to enhance the presentation of neutralizing epitopes to target antibody responses to protective epitopes are strongly warranted.

In addition to neutralizing antibody responses, results from
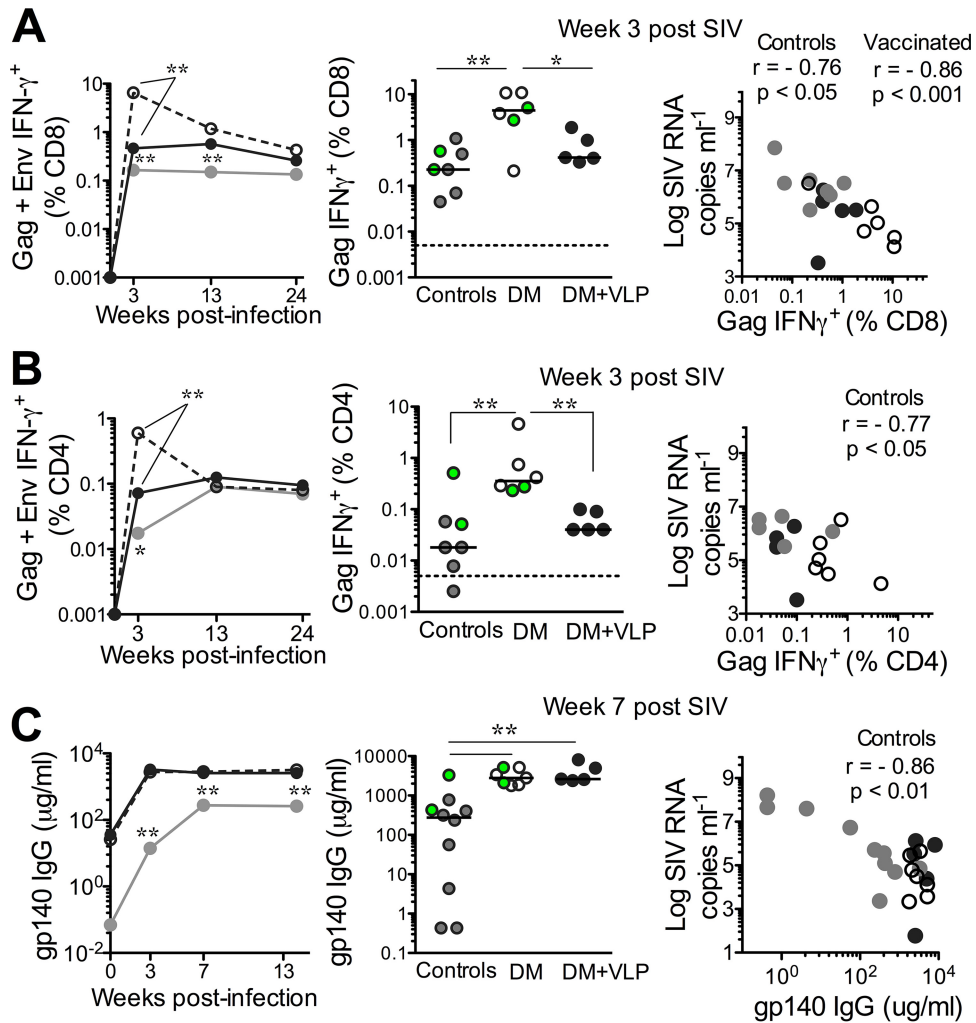
FIG 8 Immune correlates of viral control. (A) Kinetics of SIV-specific CD8 T cell responses following infection. The magnitude of the Gag-specific CD8 T cell response at week 3 postinfection correlates inversely with the viral load at week 3 (**, $P < 0.01$; *, $P < 0.05$). (B) Kinetics of SIV-specific CD4 T cell responses following infection. The magnitude of Gag-specific CD4 T cell responses at week 3 correlates inversely with the viral load at week 3 in unvaccinated controls (**, $P < 0.01$; *, $P < 0.05$). (C) Kinetics of gp140-specific antibody titers following infection. The magnitude of titers at week 7 correlates inversely with the week 7 viral load in unvaccinated controls (**, $P < 0.01$). Kinetic data are shown as median values for each group.

the RV144 trial and several nonhuman primate vaccine efficacy studies have underscored the importance of nonneutralizing functional antibodies in mediating protection (37). Serum antibody-dependent cell-mediated cytotoxicity (ADCC) titers were inversely associated with the risk of infection in RV144 vaccinees with low Env-specific IgA titers in sera (3, 38). On the other hand, ADP responses measured 2 weeks following the final boost in RV144 vaccinees were not detected (39). In monkey studies, ADP responses have been shown to be protective (37). We did not observe a significant association of ADP in sera and acquisition in our study. It is possible that ADP activities in rectal secretions may be more discriminating. Further research on antibody effector functions at the mucosal portals in the setting of immunizations with a DNA prime/poxvirus vector plus a protein boost is strongly warranted.

To gauge the synergy of the VLP protein boost with DNA/MVA vaccines, we compared our results to those of a parallel study by the Pulendran laboratory investigating the immunoge-

nicity of four homologous VLP prime-boost immunizations identical in formulation, amount, and delivery to the VLP boost used in the present study (Kasturi SP, Kozlowski PA, Nakaya HI, Burger MC, Russo P, Pham M, Kovalenkov Y, Silveira ELV, Havenar-Daughton C, Burton SL, Kilgore KM, Johnson MJ, Nabi R, Legere T, Sher ZJ, Chen X, Amara RR, Hunter E, Bosinger SE, Spearman P, Crotty S, Villinger F, Derdeyn CA, Wrammert J, and Pulendran B, unpublished data). The data showed that mucosal SIV Env-specific IgG titers elicited by the VLP boost following DNA/MVA vaccination were up to 10-fold higher at peak and memory time points than those following a homologous VLP prime-boost. These results demonstrate that VLP immunogens are more efficient in boosting an anti-Env antibody response in a heterologous than in a homologous prime-boost regimen. In addition, a pure trimeric gp140 protein may be more effective in boosting Env-specific antibody titers (40). Furthermore, a longer follow-up time after protein boost will provide a better assessment of the persistence of titers and the value of extended boost regimens.

Our data call attention to effective boosting of CD8 T cell responses to achieve optimal viral control in the event of breakthrough infections. VLP immunization did not boost DNA/MVA-induced memory CD8 T cells. Correspondingly, VLP-boosted animals showed, on average, lower frequencies of Gag-specific CD8 T cells at the peak time point postinfection. It is possible that the longer time interval between the final MVA immunization and challenge in VLP-boosted animals contributed to the slower recall of Gag-specific CD8 T cells, which in turn favored viral replication. These data underscore the importance of the optimal engagement of CD8 T cells by combining a viral vector with protein immunogens during extended boosts to achieve robust acute virus control.

In conclusion, the present studies demonstrate the ability of a late VLP protein boost to elicit a strong recall of Env antibody responses in sera and mucosa. Boosting with gp160 altered the epitope specificity but did not result in broad neutralization. The data support a role for a synergistic effect of a late VLP protein boost in vaccine efficacy, with 2/7 VLP-boosted animals resisting a highly stringent SIVmac251 challenge, compared to 0/7 animals in DM group. Novel Env immunogens which elicit broadly neutralizing antibody responses are likely to synergize well with DNA/MVA vaccines and improve and augment vaccine immunogenicity and vaccine efficacy.

REFERENCES

1. **Fauci AS, Folkers GK, Marston HD.** 2014. Ending the global HIV/AIDS pandemic: the critical role of an HIV vaccine. Clin Infect Dis **59**(Suppl 2):S80–S84. http://dx.doi.org/10.1093/cid/ciu420.

2. **Rerks-Ngarm S, Pitisuttithum P, Nitayaphan S, Kaewkungwal J, Chiu J, Paris R, Premsri N, Namwat C, de Souza M, Adams E, Benenson M, Gurunathan S, Tartaglia J, McNeil JG, Francis DP, Stablein D, Birx DL, Chunsuttiwat S, Khamboonruang C, Thongcharoen P, Robb ML, Michael NL, Kunasol P, Kim JH.** 2009. Vaccination with ALVAC and AIDSVAX to prevent HIV-1 infection in Thailand. N Engl J Med **361:** 2209–2220. http://dx.doi.org/10.1056/NEJMoa0908492.

3. **Kim JH, Excler JL, Michael NL.** 2015. Lessons from the RV144 Thai phase III HIV-1 vaccine trial and the search for correlates of protection. Annu Rev Med **66:**423–437. http://dx.doi.org/10.1146/annurev-med -052912-123749.

4. **Esparza J.** 2013. A brief history of the global effort to develop a preventive HIV vaccine. Vaccine **31:**3502–3518. http://dx.doi.org/10.1016/j.vaccine .2013.05.018.

5. **Corey L, Gilbert PB, Tomaras GD, Haynes BF, Pantaleo G, Fauci AS.** 2015. Immune correlates of vaccine protection against HIV-1 acquisition. Sci Transl Med **7:**310rv7. http://dx.doi.org/10.1126/scitranslmed .aac7732.

6. **Pascutti MF, Rodriguez AM, Falivene J, Giavedoni L, Drexler I, Gherardi MM.** 2011. Interplay between modified vaccinia virus Ankara and dendritic cells: phenotypic and functional maturation of bystander dendritic cells. J Virol **85:**5532–5545. http://dx.doi.org/10.1128/JVI.02267-10.

7. **Liu L, Chavan R, Feinberg MB.** 2008. Dendritic cells are preferentially targeted among hematolymphocytes by modified vaccinia virus Ankara and play a key role in the induction of virus-specific T cell responses in vivo. BMC Immunol **9:**15. http://dx.doi.org/10.1186/1471-2172-9-15.

8. **Robinson HL, Sharma S, Zhao J, Kannanganat S, Lai L, Chennareddi L, Yu T, Montefiori DC, Amara RR, Wyatt LS, Moss B.** 2007. Immunogenicity in macaques of the clinical product for a clade B DNA/MVA HIV vaccine: elicitation of IFN-gamma, IL-2, and TNF-alpha coproducing CD4 and CD8 T cells. AIDS Res Hum Retroviruses **23:**1555–1562. http: //dx.doi.org/10.1089/aid.2007.0165.

9. **Goepfert PA, Elizaga ML, Sato A, Qin L, Cardinali M, Hay CM, Hural J, DeRosa SC, DeFawe OD, Tomaras GD, Montefiori DC, Xu Y, Lai L, Kalams SA, Baden LR, Frey SE, Blattner WA, Wyatt LS, Moss B, Robinson HL.** 2011. Phase 1 safety and immunogenicity testing of DNA and recombinant modified vaccinia Ankara vaccines expressing HIV-1 virus-like particles. J Infect Dis **203:**610–619. http://dx.doi.org/10.1093 /infdis/jiq105.

10. **Goepfert PA, Elizaga ML, Seaton K, Tomaras GD, Montefiori DC, Sato A, Hural J, DeRosa SC, Kalams SA, McElrath MJ, Keefer MC, Baden LR, Lama JR, Sanchez J, Mulligan MJ, Buchbinder SP, Hammer SM, Koblin BA, Pensiero M, Butler C, Moss B, Robinson HL.** 2014. Specificity and 6-month durability of immune responses induced by DNA and recombinant modified vaccinia Ankara vaccines expressing HIV-1 virus-like particles. J Infect Dis **210:**99–110. http://dx.doi.org/10.1093/infdis /jiu003.

11. **Sanders RW, van Gils MJ, Derking R, Sok D, Ketas TJ, Burger JA, Ozorowski G, Cupo A, Simonich C, Goo L, Arendt H, Kim HJ, Lee JH, Pugach P, Williams M, Debnath G, Moldt B, van Breemen MJ, Isik G, Medina-Ramirez M, Back JW, Koff WC, Julien JP, Rakasz EG, Seaman MS, Guttman M, Lee KK, Klasse PJ, LaBranche C, Schief WR, Wilson IA, Overbaugh J, Burton DR, Ward AB, Montefiori DC, Dean H, Moore JP.** 2015. HIV-1 vaccines. HIV-1 neutralizing antibodies induced by native-like envelope trimers. Science **349:**aac4223. http://dx.doi.org/10 .1126/science.aac4223.

12. **de Taeye SW, Ozorowski G, Torrents de la Pena A, Guttman M, Julien JP, van den Kerkhof TL, Burger JA, Pritchard LK, Pugach P, Yasmeen A, Crampton J, Hu J, Bontjer I, Torres JL, Arendt H, DeStefano J, Koff WC, Schuitemaker H, Eggink D, Berkhout B, Dean H, LaBranche C, Crotty S, Crispin M, Montefiori DC, Klasse PJ, Lee KK, Moore JP, Wilson IA, Ward AB, Sanders RW.** 2015. Immunogenicity of stabilized HIV-1 envelope trimers with reduced exposure of non-neutralizing epitopes. Cell **163:**1702–1715. http://dx .doi.org/10.1016/j.cell.2015.11.056.

13. **National Research Council.** 2011. Guide for the care and use of laboratory animals, 8th ed. National Academies Press, Washington, DC.

14. **Kwa S, Lai L, Gangadhara S, Siddiqui M, Pillai VB, Labranche C, Yu T, Moss B, Montefiori DC, Robinson HL, Kozlowski PA, Amara RR.** 2014. CD40L-adjuvanted DNA/modified vaccinia virus Ankara simian immunodeficiency virus SIV239 vaccine enhances SIV-specific humoral and cellular immunity and improves protection against a heterologous SIVE660 mucosal challenge. J Virol **88:**9579–9589. http://dx.doi.org/10 .1128/JVI.00975-14.

15. **Amara RR, Villinger F, Altman JD, Lydy SL, O'Neil SP, Staprans SI, Montefiori DC, Xu Y, Herndon JG, Wyatt LS, Candido MA, Kozyr NL, Earl PL, Smith JM, Ma HL, Grimm BD, Hulsey ML, McClure HM, McNicholl JM, Moss B, Robinson HL.** 2002. Control of a mucosal challenge and prevention of AIDS by a multiprotein DNA/ MVA vaccine. Vaccine **20:**1949–1955. http://dx.doi.org/10.1016 /S0264-410X(02)00076-2.

16. **Van Rompay KK, Greenier JL, Cole KS, Earl P, Moss B, Steckbeck JD, Pahar B, Rourke T, Montelaro RC, Canfield DR, Tarara RP, Miller C, McChesney MB, Marthas ML.** 2003. Immunization of newborn rhesus macaques with simian immunodeficiency virus (SIV) vaccines prolongs

survival after oral challenge with virulent SIVmac251. J Virol **77:**179–190. http://dx.doi.org/10.1128/JVI.77.1.179-190.2003.

17. Kozlowski PA, Lynch RM, Patterson RR, Cu-Uvin S, Flanigan TP, Neutra MR. 2000. Modified wick method using Weck-Cel sponges for collection of human rectal secretions and analysis of mucosal HIV antibody. J Acquir Immune Defic Syndr **24:**297–309. http://dx.doi.org/10.1097/00042560-200008010-00001.

18. Shen X, Duffy R, Howington R, Cope A, Sadagopal S, Park H, Pal R, Kwa S, Ding S, Yang OO, Fouda GG, Le Grand R, Bolton D, Esteban M, Phogat S, Roederer M, Amara RR, Picker LJ, Seder RA, McElrath MJ, Barnett S, Permar SR, Shattock R, DeVico AL, Felber BK, Pavlakis GN, Pantaleo G, Korber BT, Montefiori DC, Tomaras GD. 2015. Vaccine-induced linear epitope-specific antibodies to simian immunodeficiency virus SIVmac239 envelope are distinct from those induced to the human immunodeficiency virus type 1 envelope in nonhuman primates. J Virol **89:**8643–8650. http://dx.doi.org/10.1128/JVI.03635-14.

19. Imholte GC, Sauteraud R, Korber B, Bailer RT, Turk ET, Shen X, Tomaras GD, Mascola JR, Koup RA, Montefiori DC, Gottardo R. 2013. A computational framework for the analysis of peptide microarray antibody binding data with application to HIV vaccine profiling. J Immunol Methods **395:**1–13. http://dx.doi.org/10.1016/j.jim.2013.06.001.

20. Iyer SS, Gangadhara S, Victor B, Gomez R, Basu R, Hong JJ, Labranche C, Montefiori DC, Villinger F, Moss B, Amara RR. 2015. Codelivery of envelope protein in alum with MVA vaccine induces CXCR3-biased CXCR5$^+$ and CXCR5$^-$ CD4 T cell responses in rhesus macaques. J Immunol **195:**994–1005. http://dx.doi.org/10.4049/jimmunol.1500083.

21. Lai L, Vodros D, Kozlowski PA, Montefiori DC, Wilson RL, Akerstrom VL, Chennareddi L, Yu T, Kannanganat S, Ofielu L, Villinger F, Wyatt LS, Moss B, Amara RR, Robinson HL. 2007. GM-CSF DNA: an adjuvant for higher avidity IgG, rectal IgA, and increased protection against the acute phase of a SHIV-89.6P challenge by a DNA/MVA immunodeficiency virus vaccine. Virology **369:**153–167. http://dx.doi.org/10.1016/j.virol.2007.07.017.

22. Kannanganat S, Nigam P, Velu V, Earl PL, Lai L, Chennareddi L, Lawson B, Wilson RL, Montefiori DC, Kozlowski PA, Moss B, Robinson HL, Amara RR. 2010. Preexisting vaccinia virus immunity decreases SIV-specific cellular immunity but does not diminish humoral immunity and efficacy of a DNA/MVA vaccine. J Immunol **185:**7262–7273. http://dx.doi.org/10.4049/jimmunol.1000751.

23. Tomaras GD, Yates NL, Liu P, Qin L, Fouda GG, Chavez LL, Decamp AC, Parks RJ, Ashley VC, Lucas JT, Cohen M, Eron J, Hicks CB, Liao HX, Self SG, Landucci G, Forthal DN, Weinhold KJ, Keele BF, Hahn BH, Greenberg ML, Morris L, Karim SS, Blattner WA, Montefiori DC, Shaw GM, Perelson AS, Haynes BF. 2008. Initial B-cell responses to transmitted human immunodeficiency virus type 1: virion-binding immunoglobulin M (IgM) and IgG antibodies followed by plasma anti-gp41 antibodies with ineffective control of initial viremia. J Virol **82:**12449–12463. http://dx.doi.org/10.1128/JVI.01708-08.

24. Gordon SN, Doster MN, Kines RC, Keele BF, Brocca-Cofano E, Guan Y, Pegu P, Liyanage NP, Vaccari M, Cuburu N, Buck CB, Ferrari G, Montefiori D, Piatak M, Jr, Lifson JD, Xenophontos AM, Venzon D, Robert-Guroff M, Graham BS, Lowy DR, Schiller JT, Franchini G. 14 November 2014. Antibody to the gp120 V1/V2 loops and CD4$^+$ and CD8$^+$ T responses in protection from SIVmac251 vaginal acquisition and persistent viremia. J Immunol http://dx.doi.org/10.4049/jimmunol.1401504.

25. Kodama T, Mori K, Kawahara T, Ringler DJ, Desrosiers RC. 1993. Analysis of simian immunodeficiency virus sequence variation in tissues of rhesus macaques with simian AIDS. J Virol **67:**6522–6534.

26. Manrique M, Kozlowski PA, Wang SW, Wilson RL, Micewicz E, Montefiori DC, Mansfield KG, Carville A, Aldovini A. 2009. Nasal DNA-MVA SIV vaccination provides more significant protection from progression to AIDS than a similar intramuscular vaccination. Mucosal Immunol **2:**536–550. http://dx.doi.org/10.1038/mi.2009.103.

27. Montefiori DC. 2005. Evaluating neutralizing antibodies against HIV, SIV, and SHIV in luciferase reporter gene assays. Curr Protoc Immunol Chapter 12:Unit 12.11. http://dx.doi.org/10.1002/0471142735.im1211s64.

28. Ackerman ME, Moldt B, Wyatt RT, Dugast AS, McAndrew E, Tsoukas S, Jost S, Berger CT, Sciaranghella G, Liu Q, Irvine DJ, Burton DR, Alter G. 2011. A robust, high-throughput assay to determine the phagocytic activity of clinical antibody samples. J Immunol Methods **366:**8–19. http://dx.doi.org/10.1016/j.jim.2010.12.016.

29. Tuero I, Mohanram V, Musich T, Miller L, Vargas-Inchaustegui DA, Demberg T, Venzon D, Kalisz I, Kalyanaraman VS, Pal R, Ferrari MG, LaBranche C, Montefiori DC, Rao M, Vaccari M, Franchini G, Barnett SW, Robert-Guroff M. 2015. Mucosal B cells are associated with delayed SIV acquisition in vaccinated female but not male rhesus macaques following SIVmac251 rectal challenge. PLoS Pathog **11:**e1005101. http://dx.doi.org/10.1371/journal.ppat.1005101.

30. Robb ML, Rerks-Ngarm S, Nitayaphan S, Pitisuttithum P, Kaewkungwal J, Kunasol P, Khamboonruang C, Thongcharoen P, Morgan P, Benenson M, Paris RM, Chiu J, Adams E, Francis D, Gurunathan S, Tartaglia J, Gilbert P, Stablein D, Michael NL, Kim JH. 2012. Risk behaviour and time as covariates for efficacy of the HIV vaccine regimen ALVAC-HIV (vCP1521) and AIDSVAX B/E: a post-hoc analysis of the Thai phase 3 efficacy trial RV 144. Lancet Infect Dis **12:**531–537. http://dx.doi.org/10.1016/S1473-3099(12)70088-9.

31. Kasturi SP, Skountzou I, Albrecht RA, Koutsonanos D, Hua T, Nakaya HI, Ravindran R, Stewart S, Alam M, Kwissa M, Villinger F, Murthy N, Steel J, Jacob J, Hogan RJ, Garcia-Sastre A, Compans R, Pulendran B. 2011. Programming the magnitude and persistence of antibody responses with innate immunity. Nature **470:**543–547. http://dx.doi.org/10.1038/nature09737.

32. Li H, Stephenson KE, Kang ZH, Lavine CL, Seaman MS, Barouch DH. 2014. Common features of mucosal and peripheral antibody responses elicited by candidate HIV-1 vaccines in rhesus monkeys. J Virol **88:**13510–13515. http://dx.doi.org/10.1128/JVI.02095-14.

33. Wyand MS, Manson KH, Garcia-Moll M, Montefiori D, Desrosiers RC. 1996. Vaccine protection by a triple deletion mutant of simian immunodeficiency virus. J Virol **70:**3724–3733.

34. Zolla-Pazner S, deCamp A, Gilbert PB, Williams C, Yates NL, Williams WT, Howington R, Fong Y, Morris DE, Soderberg KA, Irene C, Reichman C, Pinter A, Parks R, Pitisuttithum P, Kaewkungwal J, Rerks-Ngarm S, Nitayaphan S, Andrews C, O'Connell RJ, Yang ZY, Nabel GJ, Kim JH, Michael NL, Montefiori DC, Liao HX, Haynes BF, Tomaras GD. 2014. Vaccine-induced IgG antibodies to V1V2 regions of multiple HIV-1 subtypes correlate with decreased risk of HIV-1 infection. PLoS One **9:**e87572. http://dx.doi.org/10.1371/journal.pone.0087572.

35. Pegu P, Vaccari M, Gordon S, Keele BF, Doster M, Guan Y, Ferrari G, Pal R, Ferrari MG, Whitney S, Hudacik L, Billings E, Rao M, Montefiori D, Tomaras G, Alam SM, Fenizia C, Lifson JD, Stablein D, Tartaglia J, Michael N, Kim J, Venzon D, Franchini G. 2013. Antibodies with high avidity to the gp120 envelope protein in protection from simian immunodeficiency virus SIV(mac251) acquisition in an immunization regimen that mimics the RV-144 Thai trial. J Virol **87:**1708–1719. http://dx.doi.org/10.1128/JVI.02544-12.

36. Gordon SN, Doster MN, Kines RC, Keele BF, Brocca-Cofano E, Guan Y, Pegu P, Liyanage NP, Vaccari M, Cuburu N, Buck CB, Ferrari G, Montefiori D, Piatak M, Jr, Lifson JD, Xenophontos AM, Venzon D, Robert-Guroff M, Graham BS, Lowy DR, Schiller JT, Franchini G. 2014. Antibody to the gp120 V1/V2 loops and CD4$^+$ and CD8$^+$ T cell responses in protection from SIVmac251 vaginal acquisition and persistent viremia. J Immunol **193:** 6172–6183. http://dx.doi.org/10.4049/jimmunol.1401504.

37. Barouch DH, Stephenson KE, Borducchi EN, Smith K, Stanley K, McNally AG, Liu J, Abbink P, Maxfield LF, Seaman MS, Dugast AS, Alter G, Ferguson M, Li W, Earl PL, Moss B, Giorgi EE, Szinger JJ, Eller LA, Billings EA, Rao M, Tovanabutra S, Sanders-Buell E, Weijtens M, Pau MG, Schuitemaker H, Robb ML, Kim JH, Korber BT, Michael NL. 2013. Protective efficacy of a global HIV-1 mosaic vaccine against heterologous SHIV challenges in rhesus monkeys. Cell **155:**531–539. http://dx.doi.org/10.1016/j.cell.2013.09.061.

38. Tomaras GD, Ferrari G, Shen X, Alam SM, Liao HX, Pollara J, Bonsignori M, Moody MA, Fong Y, Chen X, Poling B, Nicholson CO, Zhang R, Lu X, Parks R, Kaewkungwal J, Nitayaphan S, Pitisuttithum P, Rerks-Ngarm S, Gilbert PB, Kim JH, Michael NL, Montefiori DC, Haynes BF. 2013. Vaccine-induced plasma IgA specific for the C1 region of the HIV-1 envelope blocks binding and effector function of IgG. Proc Natl Acad Sci U S A **110:**9019–9024. http://dx.doi.org/10.1073/pnas.1301456110.

39. Ana-Sosa-Batiz F, Johnston AP, Liu H, Center RJ, Rerks-Ngarm S, Pitisuttithum P, Nitayaphan S, Kaewkungwal J, Kim JH, Michael NL, Kelleher AD, Stratov I, Kent SJ, Kramski M. 2014. HIV-specific antibody-dependent phagocytosis matures during HIV infection. Immunol Cell Biol **92:**679–687. http://dx.doi.org/10.1038/icb.2014.42.

40. Schiller J, Chackerian B. 2014. Why HIV virions have low numbers of envelope spikes: implications for vaccine development. PLoS Pathog **10:** e1004254. http://dx.doi.org/10.1371/journal.ppat.1004254.